Guidance and Nonlinear Active Fault Tolerant Control for General Aviation Aircraft

G. Bertoni*, P.Castaldi*, N. Bertozzi*,
M. Bonfè, and S. Simani****

**University of Bologna, II Faculty of Engineering, Italy*
(Tel/Fax: +39-0543-786934; e-mail: gianni.bertoni, paolo.castaldi@unibo.it)
***University of Ferrara, Department of Engineering , Italy*

Abstract: This paper addresses the development of a novel Active Fault Tolerant Control Scheme (AFTCS) which, when used with an independently designed guidance system, turns out to give an overall fault tolerant guidance and control system. This AFTCS methodology avoids a logic-based switching controller by exploiting an adaptive fault estimator whose design is based on the Non Linear Geometric Approach (NLGA). The application of the AFTC scheme to a Piper PA-30 aircraft simulator in a flight condition characterized by a tight-coupled longitudinal and lateral dynamics even in presence of wind, shows the enhancement of the flying quality, the asymptotic fault accommodation and the control objective recovery.

Keywords: fault detection and diagnosis, active fault tolerant control, adaptive filter, nonlinear geometric approach.

1. INTRODUCTION

A conventional feedback control design for a complex system may result in an unsatisfactory performance, or even instability, in the event of malfunctions in actuators, sensors or other system components. To overcome such weaknesses, new approaches to control system design have been developed in order to tolerate component malfunctions, while maintaining desirable stability and performance properties. This is particularly important for safety-critical systems, such as aircraft and spacecraft applications. In such systems, the consequences of a minor fault in a system component can be catastrophic. Therefore, the demand on reliability, safety and fault tolerance is generally high. It is necessary to design control systems which are capable of tolerating potential faults in order to improve the reliability and availability while providing a desirable performance. These types of control systems are often known as fault-tolerant control systems, which possess the ability to accommodate component faults automatically.

In general, fault tolerant control methods are classified into two types, i.e. Passive Fault Tolerant Control Scheme (PFTCS), and Active Fault Tolerant Control Scheme (AFTCS) (Mahmoud et al., 2003; Blanke et al., 2006, Zhang and Jiang, 2008). In a PFTCS, controllers are fixed and are designed to be robust against a class of presumed faults. This approach does not need a fault estimate (or detection) or controller reconfiguration, but only limited fault-tolerant capabilities (Mahmoud et al., 2003; Zhang and Jiang, 2008). In contrast to a PFTCS, an AFTCS reacts to the system component failures actively by reconfiguring control actions so that the stability and acceptable performance of the entire system can be maintained. An AFTCS relies heavily on real-time FDD (*Fault Detection and Diagnosis)* schemes to provide the most up-to-date information about the true status of the system. This information can be used both for a logic-based switching controller and for a feedback of the fault estimate. The approach proposed in this paper is of the latter type. Over the last three decades, the growing demand for safety, reliability, maintainability, and survivability in technical systems has led to a significant research effort in FDD developing many FDD techniques, see, for example, the survey works (Simani et al., 2002; Mahmoud et al., 2003; Blanke et al., 2006; Isermann, 2005; Witczak, 2007; Zhang and Jiang, 2008). Regarding the AFTCS design, (Zhang and Jiang, 2008) argued that, good FDD is needed. They claim that, for the system to react properly to a fault, timely and accurate detection and location of the fault itself is needed. The area where research studies have mostly been explored is the approach that leads to an Fault Detection and Isolation (FDI) scheme by means of the residual generation while FDD schemes are a challenging topic because they provide fault estimates too. FDI and FDD schemes usually exploit dynamic observers or filters. Plant-model mismatches can cause false alarms or, even worse, missed faults. Robustness issues in FDI and FDD are therefore very important (Chen and Patton, 1999; Blanke et al., 2006; Isermann, 2005; Witczak, 2007).

The present paper is focused on the development of a novel AFTCS, which integrates a reliable and robust FDD scheme together with the design of a controller reconfiguration system. In particular, the methodology is based on a FDD procedure relying on adaptive filters designed via the NonLinear Geometric Approach (NLGA). The controller reconfiguration exploits a further control loop, depending on the on-line estimate of the fault signal. One of the main advantages of this strategy is that a structure of logic-based

switching controller is not required. The novelty of the proposed AFTCS lies in the feedback of the estimated fault signal, which is obtained by the adaptive filters designed via the NLGA. The achieved simulation results show that the feeding back of the reconstructed fault signal enhances not only the fault estimate itself but also the final performances of the overall system. This paper will show the capabilities of the AFTCS to handle faults without reconfiguring the overall structure of the controller by using flight conditions and fault tests characterized by a tight-coupled longitudinal and lateral dynamics even presence of wind (see Castaldi et al., 2009). Compared with different fault tolerant approaches, see e.g. (Marcos et al., 2005), the suggested AFTCS strategy keeps good performances also with significant actuator faults, since these signals are reconstructed by the FDD logic with a good accuracy.

Concerning the FDD procedure, this paper proposes a nonlinear scheme, developed in (Castaldi et al., 2009), which provides the fault detection, isolation and size estimation. The FDD nonlinear method is based on the NonLinear Geometric Approach (NLGA) developed by De Persis and Isidori (DePersis and Isidori, 2001). By means of the NLGA disturbance decoupled Adaptive Filters (NLGA-AF) providing fault estimation are developed. The AFTCS strategy is applied to the model of a small commercial aircraft (Bonfè et al., 2006; Bonfè et al., 2007a; Bonfè et al., 2007b). In particular the flight simulator of a Piper PA-30, has been implemented in the Matlab/ Simulink environment.

The AFTCS for the PA-30 aircraft simulator has been tested in this paper in a challenging flight condition with coupled longitudinal and lateral dynamics, in the presence of actuator faults and turbulence. The achieved results in faulty conditions show the enhancement of the flying quality, the asymptotic fault accommodation, and the control objective recovery.

Finally, it is worth recalling that the AFTCS is characterized by a further feedback loop which feeds the fault estimate. Obviously, the standard strategy is to apply the AFTCS to a non fault tolerant GCS as it is done in section 4. On the other hand may be interesting to test the performances of the AFTCS in presence of a GCS which is fault tolerant by itself as it is done in section 5 where a fault tolerant GCS has been developed. Also in this case the AFTCS strategy leads to an improvement of performances, especially in the transient phase after the fault has occurred. It must be emphasized that GCS of section 5, based on Feedback Linearization as to the guidance segment, is a novel application of methods coming from robotics to aerospace applications.

Summarizing, the paper is organised as follows. Section 2 provides the description of the aircraft models used for simulation and for analytical design. Section 3 describes the design of the FDD scheme based on NLGA. The structure of the AFTCS strategy and its application with a standard guidance and control system is given in section 4. Section 5 describes the design of a GCS based on feedback linearization, as to the guidance segment, and its implementation with the proposed AFTCS strategy. Concluding remarks are summarised in Section 6

2.AIRCRAFT SIMULATION AND SYNTHESIS MODELS

In this section the aircraft models used for simulation tests and a reduced model, called *synthesis model*, used for the analytical project of the NLGA-AF and the AFTCS are described.

2.1 Simulation Model

This subsection recalls the description of the monitored aircraft, whose main parameters and variables are reported in the following Table 1.

Table 1. Nomenclature

α	angle of attack
β	angle of sideslip
p_ω	roll rate
q_ω	pitch rate
r_ω	yaw rate
ϕ	bank angle
θ	elevation angle
ψ	heading angle
n_e	engine shaft angular rate
$\begin{bmatrix} I_x & 0 & -I_{xz} \\ 0 & I_y & 0 \\ -I_{xz} & 0 & I_z \end{bmatrix}$	inertia moment matrix
V	True Air Speed (TAS)
δ_e	elevator deflection angle
δ_a	aileron deflection angle
δ_r	rudder deflection angle
δ_{th}	throttle aperture percentage
H	altitude
γ	flight path angle
m	airplane mass
w_u, w_v, w_w	wind components (longitudinal, lateral, vertical)

The mathematical model, which the simulation results are based on, corresponds to a PIPER PA-30 aircraft. This simulation model relies on the classical nonlinear 6 Degrees of Freedom (DoF) rigid-body formulation (Stevens and Lewis, 2003). A set of local approximations of aerodynamic, thrust and gravitational forces has been computed and scheduled depending on the values assumed by true air speed (TAS), flap, altitude, curve radius and flight-path angle. In this way, it is possible to obtain a mathematical model for each flight condition. The aerodynamic actions are implemented by means of cubic splines approximating the nonlinear experimental curves due to the wind tunnel experimental data (Fink and Freeman, 1969; Koziol, 1971). The propulsion system consisting of two 4-pistons aspirated engines is included in the aircraft model (Bonfè et al., 2006). The relation describing the engine power loss with the altitude is also implemented and can be found in Ojha (1995).

Finally, the parameters of both the aircraft 6 DoF dynamics and the engine model can be derived from Fink and Freeman (1969) and Koziol (1971). In the simulation model are also included models of servo actuators.

A mathematical description of wind gusts as three independent air velocity components, w_u, w_v, w_w along aircraft body axes has been also considered, according to the 'discrete wind gust' formulation given in Moorhouse and Woodcock (1980). The adopted model is based on the '1-cosine' shape with a gust magnitude of $3\,m/s$ and a gust length equal to the turbulence scale length in the Dryden formulation $533.4m$.

2.2 Aircraft Synthesis Model

The aircraft simulation model has been further used as reference, in order to obtain a simplified aircraft model which can be adopted in the synthesis of the proposed NLGA AF and AFTC schemes: the *aircraft synthesis model*. In particular the above mentioned NLGA-AF scheme, described in Section 3, requires a nonlinear input affine system (see De Persis and Isidori, 2001) of type

$$\begin{cases} \dot{x} &= n(x) + g(x)u + l(x)f + p(x)d \\ y &= h(x) \end{cases} \tag{1}$$

in which the state vector $x(t) \in X$ (an open subset of $\mathbb{R}^{\ell_n}$), $u(t) \in \mathbb{R}^{\ell_u}$ is the control input vector, $f(t) \in \mathbb{R}$ is the fault, $d(t) \in \mathbb{R}^{\ell_d}$ is the disturbance vector (embedding also the faults which have to be decoupled, in order to perform the fault isolation) and $y(t) \in \mathbb{R}^{\ell_m}$ the output vector, whilst $n(x)$, $l(x)$, the columns of $g(x)$ and $p(x)$ are smooth vector fields, and $h(x)$ is a smooth map. Unfortunately, the adopted simulation model of the aircraft does not fulfil this requirement For this reason, it is used a simplified aircraft model in the form of (see appendix A) model (30) .This model has been obtained on the basis of some assumptions. In particular, the expressions of aerodynamic forces and moments have been represented by means of series expansions in the neighborhood of the steady-state flight condition, then only the main terms are considered. The engine model has been simplified by linearising the power with respect to the angular rate in the neighborhood of the trim point. The second order coupling between the longitudinal and lateral--directional dynamics have been neglected. The x-body axis component of the wind has been neglected. In fact, the aircraft behavior is much more sensitive to the y-body and z-body axis wind components. Finally, the rudder effect in the equation describing the β dynamics has been neglected. It is worth noting that in Section 4 and 5 it will be shown that the designs and the simulations of the NLGA adaptive filters are robust with respect to the last approximation. In fact, the model of the β dynamics will never be used.

3. THE FDD DESIGN: NLGA ADAPTIVE FILTERS

The design of NLGA-AF to obtain an FDD scheme is based on a equivalent representation of model (30) highlighting a subsystem affected by the fault and decoupled by the disturbances. This representation is obtained by a coordinate change in the state space obtainable by means of the procedure described in the following.

By denoting with P the distribution spanned by the columns of $p(x)$, the NLGA procedure can be stated as follows:

1. determine the minimal conditioned invariant distribution containing P (denoted with Σ_P^*)
2. by using $(\Sigma_P^*)^{\perp}$, i.e. the maximal conditioned invariant codistribution contained in $P^{\perp}$, determine the largest observability codistribution contained in $P^{\perp}$ (denoted with Ω^*)
3. if $l(x) \notin (\Omega^*)^{\perp}$ continue to the next step, otherwise the fault is not detectable;
4. if the condition at step 3 is satisfied, both a surjection Ψ_1 and a function Φ_1 can be found such that $\Omega^* \cap \text{span}\{dh\} = \text{span}\{d(\Psi_1 \circ h)\}$ and $\Omega^* = \text{span}\{d(\Phi_1)\}$;

$$\begin{cases} \Psi(y) &= \begin{pmatrix} \overline{y}_1 \\ \overline{y}_2 \end{pmatrix} = \begin{pmatrix} \Psi_1(y) \\ H_2 y \end{pmatrix} \\ \Phi(x) &= \begin{pmatrix} \overline{x}_1 \\ \overline{x}_2 \\ \overline{x}_3 \end{pmatrix} = \begin{pmatrix} \Phi_1(x) \\ H_2 h(x) \\ \Phi_3(x) \end{pmatrix} \end{cases} \tag{2}$$

are (local) diffeomorphisms (H_2 is a selection matrix, ie. its rows are a subset of the rows of the identity matrix) .

By adopting the new (local) state and output coordinates $(\overline{x}, \overline{y})$, the system (1)is described as follows

$$\begin{cases} \dot{\overline{x}}_1 &= n_1(\overline{x}_1, \overline{x}_2) + g_1(\overline{x}_1, \overline{x}_2)c + \ell_1(\overline{x}_1, \overline{x}_2, \overline{x}_3)f \\ \dot{\overline{x}}_2 &= n_2(\overline{x}_1, \overline{x}_2, \overline{x}_3) + g_2(\overline{x}_1, \overline{x}_2, \overline{x}_3)c + \\ &\quad + \ell_2(\overline{x}_1, \overline{x}_2, \overline{x}_3)f + p_2(\overline{x}_1, \overline{x}_2, \overline{x}_3)d \\ \dot{\overline{x}}_3 &= n_3(\overline{x}_1, \overline{x}_2, \overline{x}_3) + g_3(\overline{x}_1, \overline{x}_2, \overline{x}_3)c + \\ &\quad + \ell_3(\overline{x}_1, \overline{x}_2, \overline{x}_3)f + p_3(\overline{x}_1, \overline{x}_2, \overline{x}_3)d \\ y_1 &= h(\overline{x}_1) \\ y_2 &= \overline{x}_2 \end{cases} \tag{3}$$

with $\ell_1(\overline{x}_1, \overline{x}_2, \overline{x}_3)$ not identically zero. It is worth observing that $\overline{x}_2$ is measured, so that by denoting with $\overline{x}_2$ with $\overline{y}_2$ and

considering it as an independent input, the following $\overline{x}_1$-subsystem can be singled out

$$\begin{cases} \dot{\overline{x}}_1 &= n_1\left(\overline{x}_1, \overline{y}_2\right) + g_1\left(\overline{x}_1, \overline{y}_2\right)c + \ell_1\left(\overline{x}_1, \overline{y}_2, \overline{x}_3\right)f \\ \overline{y}_1 &= h\left(\overline{x}_1\right) \end{cases} \quad (4)$$

which is affected by the fault and decoupled from the disturbances. Moreover in our application $\overline{x}_3$ it is not present because the whole state is measured. Subsystem (4) can be exploited for the design of the adaptive filters estimating the fault f.

Remark 1 *The new proposed FDI scheme can be applied only if the fault detectability condition holds and the following new constraints are satisfied:*

- *the x_1–subsystem (4) is independent from the $\overline{x}_3$ state components;*
- *the fault is a step function of the time, hence the parameter f is a constant to be estimated*
- *there exists a proper scalar component $\overline{x}_{1s}$ of the state vector $\overline{x}_1$ such that the corresponding scalar component of the output vector is $\overline{y}_{1s} = \overline{x}_{1s}$ and the following relation holds* (Castaldi et al., 2009)

$$\dot{\overline{y}}_{1s}(t) = M_1(t)\cdot f + M_2(t) \quad (5)$$

where $M_1(t) \neq 0, \forall t \geq 0$. Moreover $M_1(t)$ and $M_2(t)$ can be computed for each time instant, since they are functions just of input and output measurements. The relation (5) describes the general form of the system under diagnosis

Problem 1 *The design of an adaptive filter is required, with reference to the system model* (5)*, in order to perform an estimation $\hat{f}(t)$, which asymptotically converges to the magnitude of the fault f.*

The proposed adaptive filter that solves the FDI Problem 1 is based on the least-squares algorithm with forgetting factor (Ioannou and Sun (1996)) and described by the following adaptation law:

$$\begin{cases} \dot{P} &= \beta P - \dfrac{1}{N^2}P^2\breve{M}_1^2, & P\left(0\right) = P_0 > 0 \\ \dot{\hat{f}} &= P\,\epsilon\,\breve{M}_1, & \hat{f}\left(0\right) = 0 \end{cases} \quad (6)$$

with the following equations representing the output estimation and the corresponding normalised estimation error:

$$\begin{cases} \hat{\breve{y}}_{1s} &= \breve{M}_1\,\hat{f} + \breve{M}_2 + \lambda\,\breve{\overline{y}}_{1s} \\ \epsilon &= \dfrac{1}{N^2}\left(\overline{y}_{1s} - \hat{\breve{y}}_{1s}\right) \end{cases} \quad (7)$$

where all the involved variables of the adaptive filter are scalar. In particular, $\lambda > 0$ is a parameter related to the bandwidth of the filter, $\beta \geq 0$ is the forgetting factor and $N^2 = 1 + \breve{M}_1^2$ is the normalisation factor of the least-squares algorithm. Moreover, the proposed adaptive filter adopts the signals $\breve{M}_1$, $\breve{M}_2$, $\breve{\overline{y}}_{1s}$ which are obtained by means of a low-pass filtering of the signals M_1, M_2, $\overline{y}_{1s}$ as follows:

$$\begin{cases} \dot{\breve{M}}_1 &= -\lambda\,\breve{M}_1 + M_1, & \breve{M}_1(0) = 0 \\ \dot{\breve{M}}_2 &= -\lambda\,\breve{M}_2 + M_2, & \breve{M}_2(0) = 0 \\ \dot{\breve{\overline{y}}}_{1s} &= -\lambda\,\breve{\overline{y}}_{1s} + \overline{y}_{1s}, & \breve{\overline{y}}_{1s}(0) = 0 \end{cases} \quad (8)$$

Lemma 1 *The considered adaptive filter is described by equations (6)-(8). The asymptotic relation between the normalised output estimation error $\epsilon(t)$ and the fault estimation error $f - \hat{f}(t)$ is the following*:

$$\lim_{t\to\infty}\epsilon(t) = \lim_{t\to\infty}\frac{\breve{M}_1(t)}{N^2(t)}\left(f - \hat{f}(t)\right) \quad (9)$$

The proof of Lemma 1 is reported in Castaldi et al. (2009).

Theorem 1 *The adaptive filter described by equations (6)-(8) represents a solution to the FDI Problem 1, so that $\hat{f}(t)$ provides an asymptotically convergent estimation of the magnitude of the step fault f.*

The proof of Theorem 1 is reported in Castaldi et al. (2009).

3.1 NLGA-AF estimation of aircraft faults

As described in the Sections 1 and 2, in order to assess the performance of the proposed FDD schemes, the aircraft simulation model is used. Unfortunately this model does not fulfil the input affine condition required for the NLGA framework. Hence the simplified synthesis nonlinear model (30) is adopted instead for the NLGA-AF design. Once the aircraft model (30) includes faults on the actuators, namely on the elevator f_{δ_a}, on the aileron f_{δ_a}, on the rudder f_{δ_r} and on the throttle $f_{\delta_{th}}$ actuators, it is possible to split the overall model into 4 distinct subsystems that can be expressed in the form (1). Each of the 4 aircraft models for FDD leads to the form (4) by means of a suitable coordinate transformation, as presented in (Castaldi et al.(2007b)). Furthermore, it is straightforward to verify that all the conditions required by the Remark 1 are satisfied. Hence, a set of 4 NLGA adaptive filters is designed in the general form (6)-(8)**.**This scheme allows to estimate the magnitude of a step fault acting on a single actuator. More in detail, for the FDD synthesis model with the fault on the elevator, as detailed in (Castaldi et al (2007b)), the state scalar component $\overline{x}_{1s}$ needed to detect f_{δ_e} is the following:

$$\overline{x}_{1s} = \overline{x}_{11} = \left(V\cos\alpha - \frac{I_y}{mt_d}q_\omega\right) \quad (10)$$

Hence, it is possible to specify the particular expression of the faulty dynamics of (5). The design of the NLGA adaptive filter (6)-(8) for f_{δ_e} is based on these dynamics:

$$\begin{cases} \dot{\overline{y}}_{1s,e} = M_{1e} \cdot f_{\delta_e} + M_{2e} \\ M_{1e} = -\dfrac{C_{\delta_e}}{m t_d} V^2 \\ M_{2e} = \dfrac{V^2}{m}\Big(-\big(C_{D0} + C_{D\alpha}\alpha + C_{D\alpha_2}\alpha^2\big)\cos\alpha + \\ \quad +\big(C_{L0} + C_{L\alpha}\alpha\big)\sin\alpha \\ \quad -\dfrac{\big(C_{m0} + C_{m\alpha}\alpha + C_{mq}q_\omega\big)}{t_d}\Big) \\ \quad -g\sin\theta - V\sin\alpha\, q_\omega - \dfrac{\big(I_z - I_x\big)}{m t_d} p_\omega r_\omega - \dfrac{C_{\delta_e}}{m t_d} V^2 \delta_e \end{cases} \tag{11}$$

It is worth observing that $M_{1e}(t) \neq 0$, $\forall\, t \geq 0$, since the aircraft air-speed $V(t)$ is always strictly positive in all the flight conditions. Regarding the FDI of the aircraft model with the faulty aileron, as detailed in Castaldi et al. (2007b), the state scalar component $\overline{x}_{1s}$ used for detecting f_{δ_a} has the following form:

$$\overline{x}_{1s} = \overline{x}_{11} = p_\omega \tag{12}$$

Hence the expression of the faulty system in the form (5) for f_{δ_a} is the following:

$$\begin{cases} \dot{\overline{y}}_{1s,a} = M_{1a} \cdot f_{\delta_a} + M_{2a} \\ M_{1a} = \dfrac{C_{\delta_a}}{I_x} V^2 \\ M_{2a} = \dfrac{\big(C_{l\beta}\beta + C_{lp}p_\omega\big)}{I_x} V^2 + \dfrac{\big(I_y - I_z\big)}{I_x} q_\omega r_\omega + \\ \quad + \dfrac{C_{\delta_a}}{I_x} V^2 \delta_a \end{cases} \tag{13}$$

Also for this case, $M_{1a}(t) \neq 0$, \$\\forall $t \geq 0$. Concerning the faulty rudder, as in Castaldi et al. (2007b), the state scalar component $\overline{x}_{1s}$ exploited for detecting f_{δ_r} is the following:

$$\overline{x}_{1s} = \overline{x}_{11} = r_\omega \tag{14}$$

The expression of the faulty dynamics (5).for f_{δ_r} have the form

$$\begin{cases} \dot{\overline{y}}_{1s,r} = M_{1r} \cdot f_{\delta_r} + M_{2r} \\ M_{1r} = \dfrac{C_{\delta_r}}{I_z} V^2 \\ M_{2r} = \dfrac{\big(C_{n\beta}\beta + C_{nr}r_\omega\big)}{I_z} V^2 + \dfrac{\big(I_x - I_y\big)}{I_z} p_\omega q_\omega + \\ \quad + \dfrac{C_{\delta_r}}{I_z} V^2 \delta_r \end{cases} \tag{15}$$

with $M_{1r}(t) \neq 0, \forall\, t \geq 0$. Finally, the state scalar component $\overline{x}_{1s}$ (Castaldi et al., 2007b) used for detecting the fault $f_{\delta_{th}}$ on the throttle is the following:

$$\overline{x}_{1s} = \overline{x}_{15} = n_e \tag{16}$$

The expression of the faulty dynamics (5) for $f_{\delta_{th}}$ is:

$$\begin{cases} \dot{\overline{y}}_{1s,th} = M_{1th} \cdot f_{\delta_{th}} + M_{2th} \\ M_{1th} = \dfrac{t_f}{n_e}\Big(t_0 + t_1 n_e\Big) \\ M_{2th} = t_n n_e^3 + \dfrac{t_f}{n_e}\Big(t_0 + t_1 n_e\Big)\delta_{th} \end{cases} \tag{17}$$

Also in this case $M_{1th}(t) \neq 0$, $\forall\, t \geq 0$, since the engine shaft angular rate $n_e(t)$ is always strictly positive in all the flight conditions. Moreover the usual characteristics of an aircraft internal--combustion engine leads to a set of coefficients t_f, t_0 and t_1 strictly positive.

Remark 2 *The full structure of the NLGA-AF is obtained by replacing the specific expressions of M_{1x}, and $\overline{y}_{1s,x}$, for each subscript $x \in \{e,a,r,th\}$, given by (11), (13), (15) and (17) into the general form of the adaptive filter described by (6), (7) and (8).*

4. THE AFTCS SCHEME

Regarding the AFTCS, the logic scheme of the integrated adaptive fault tolerant approach is shown in Fig. 1, where the following nomenclature and symbols have been used:

- u_r, reference input (*e.g.* the reference trajectory);
- u, actuated input;
- u_c, controlled input;
- NGC, Navigation and Guidance Control system;
- u_{NGC}, feedback signal from the NGC system;
- y, controlled output (\emph{e.g.} the aircraft trajectory);
- f, actuator fault;
- $\hat{f}$, estimated actuator fault.

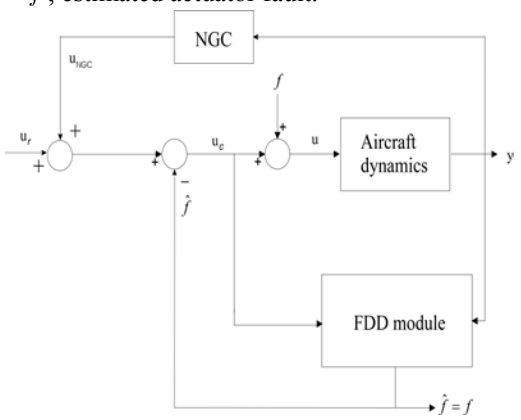

Fig. 1: Logic diagram of the integrated AFTCS strategy

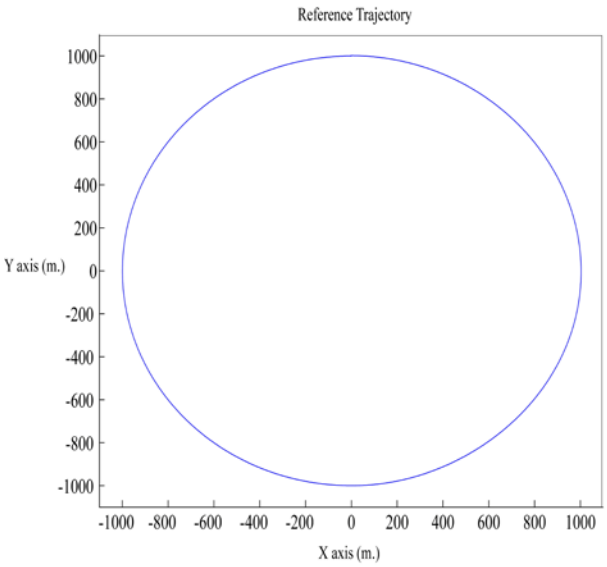

Fig. 2. Reference trajectory

Therefore, the logic scheme depicted in Fig. 1 shows how the AFTCS strategy has been implemented by integrating the FDD) module (i.e. the NLGA adaptive filters) with the existing NGC system. From the controlled input and output signals, the FDD module provides the correct estimation $\hat{f}$ of the f actuator fault, which is injected to the control loop, for compensating the effect of the actuator fault. After this correction, the current NGC module provides the exact tracking of the reference signal u_r. The simulation results proposed in this work and analytical results presented in future works, have shown that the feedback of the estimated fault $\hat{f}$ improves the identification of the fault signal f itself, by reducing also the estimation error and possible bias due to the model-system mismatch. The formal proof of the stability of the overall AFTCS will be investigated in further works. However, simulation results highlight that the aircraft state variables remain bounded in a set, which assures standard flying quality, even in the presence of large fault sizes. Moreover, the assumed fault conditions do not modify the system structure, thus guaranteeing the global stability. In Sections 4.1 and 6 will be shown the simulation results achieved by implementing the presented integrated FDD and AFTCS strategy with two different NGC systems.

4.1 SIMULATION RESULTS WITH A STANDARD NGC SYSTEM

To show the diagnostic characteristics brought by the application of the proposed integrated AFTCS and FDD schemes to the general aviation PIPER PA-30 aircraft, some simulation results are reported. The nonlinear simulation model described in section 2 has been used. A classical guidance and control system (Bonfè et al., 2006) has been used in this section. It is worth noting that this autopilot it is not fault tolerant by itself. The AFTCS will improve the behavior of the aircraft both in the transient phase and asymptotically. In order to show the capabilities of the

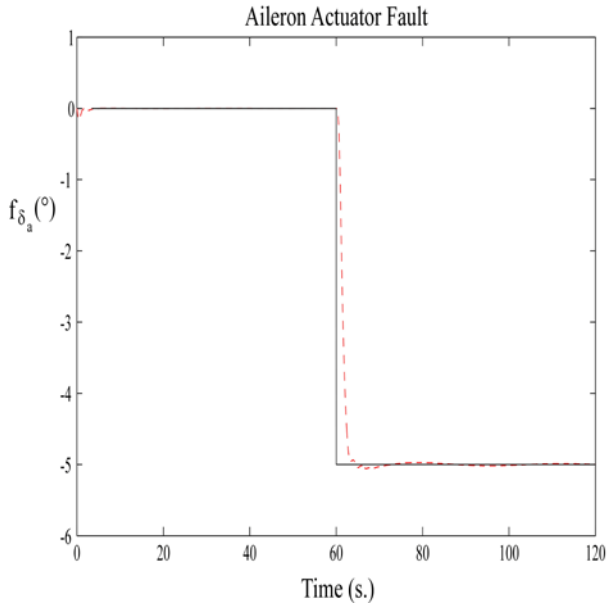

Fig. 3. Actual estimate $\hat{f}$ of f_{δ_a} aileron fault

proposed AFTCS strategy, and in particular new bias eliminating capability in estimating the actual fault f obtained by means of the feedback of the estimated fault $\hat{f}$ itself, it will be firstly considered flight conditions without turbulence. The results in presence of wind will be given too. The circular trajectory depicted in Fig. 2 has been implemented It is a coordinated turn described by the radius of curvature of 1000 m., the true air speed V of 52.36 m/s. and the altitude H of 330 m. so that 120 sec is the "turn time".

Regarding the FDD method, the NLGA adaptive filters has been used in order to perform the diagnosis and the estimation of the aileron fault size $f_{\delta_a}(t)$. It is important to note that the filter is sensitive to a single input sensor fault. The results refer to the simulation in case of actuator fault f_{δ_a} with a size of -5^o starting at time $t = 60s$.

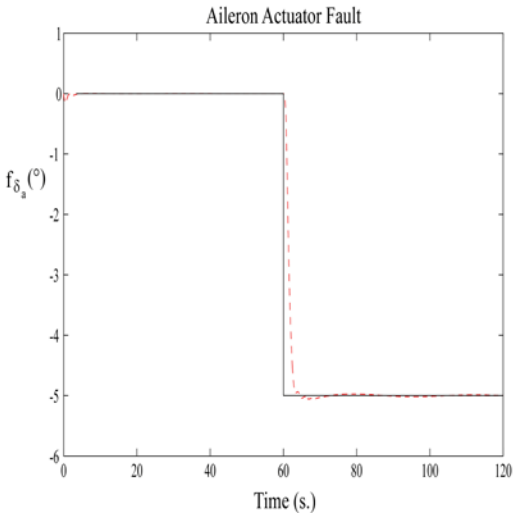

Fig. 4. Actual estimate $\hat{f}$ of f_{δ_a} aileron fault

The Fig. 3 shows the estimate $\hat{f}$ of the actuator fault (dashed line), when compared with the simulated actuator fault f_{δ_a} (continuous line). The fault estimate has been achieved by using the logic scheme represented in Fig. 1 and from the FDD module described in Section 4. It is possible to observe that the fault size of -5^o is identified correctly with a delay of about 3 s. The simulated actuator fault does not affect the aircraft stability. Note that the results are obtained by taking into account the model approximations, that are not completely de-coupled.

Figs. 4 -9 summarize some of the most meaningful aircraft variables that should assess the performances of the integrated FDD and AFTCS strategy, with and without fault recovery. The fault starting time is represented with a shaded circle. In particular, Fig. 4 shows the TAS signal V when the AFTCS recovers the fault (dashed line) and without fault accommodation (continuous line).

The Fig. 5 shows the tracking error of the aircraft with respect the reference trajectory, when the fault is recovered (dashed line) and without fault accommodation (continuous line). The tracking error is defined as the Euclidean distance between the locus of the points of the reference trajectory and the corresponding actual three-dimensional aircraft position.

Fig. 6 shows the bank angle ϕ of the aircraft with (dashed line) and without (continuous line) fault recovery. Fig. 7 depicts the angle of sideslip β of the aircraft, when the fault is recovered (dashed line) and without fault accommodation (continuous line).

On the other hand, Fig. 8 compares the trajectory of the aircraft when the fault is recovered (dashed line) and without fault accommodation (continuous line). It is clear that, the NGC system without any AFTCS would not be able to track the correct reference trajectory.

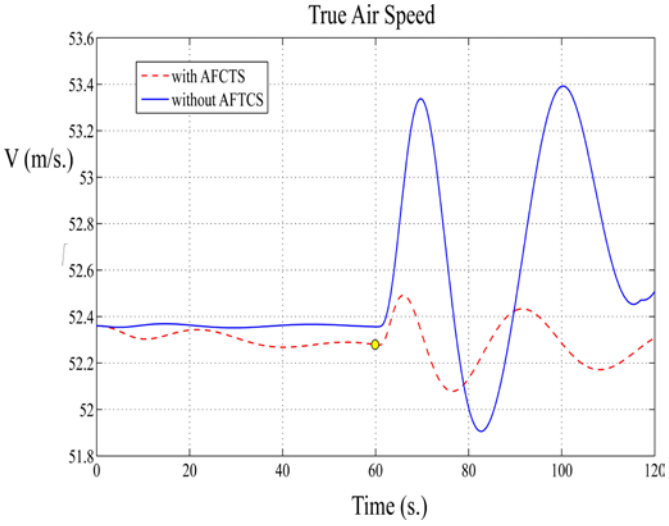

Fig. 5: True Air Speed with and without fault recovery

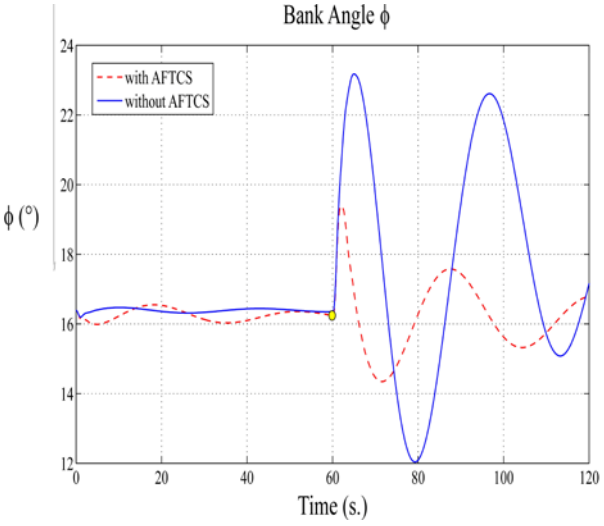

Fig. 7. Bank angle ϕ with and without fault recovery

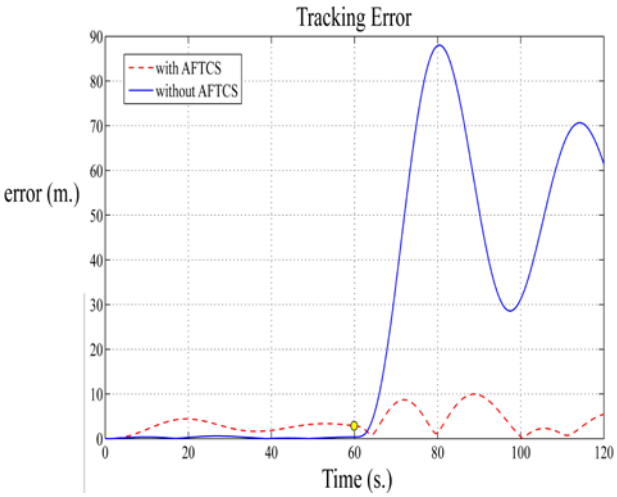

Fig. 6: Tracking error with and without fault recovery

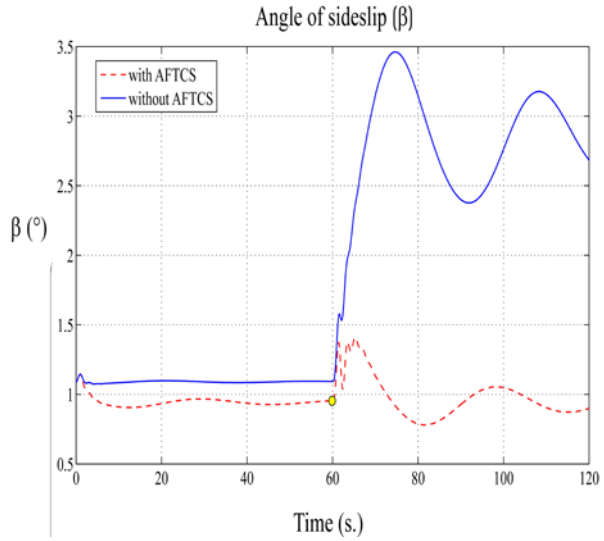

Fig. 8. Angle of sideslip β with and without fault recovery.

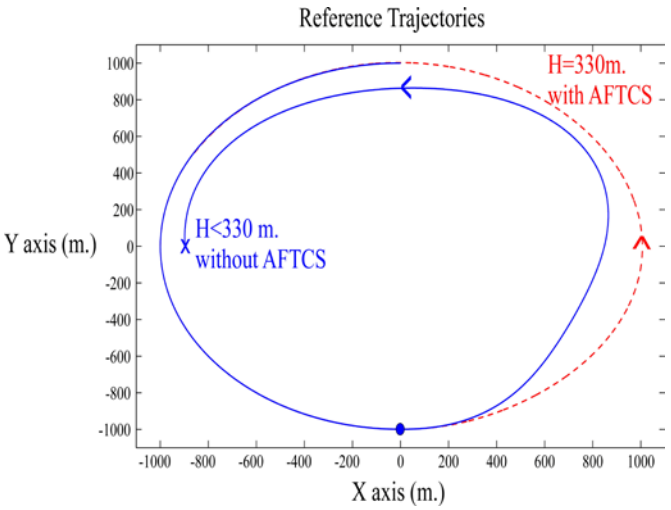

Fig. 9. Aircraft trajectory with and without fault recovery.

In Fig. 9 and Fig. 10 results in presence of turbulence are proposed. It is possible to observe the better performances of the proposed AFTCS in this case too.

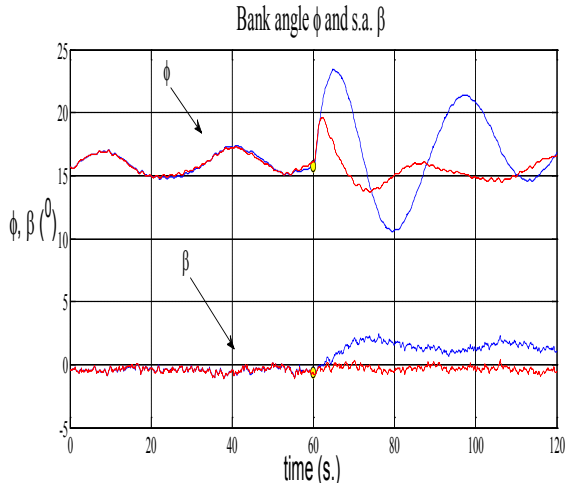

Fig. 10. Angles of bank ϕ and sideslip β with (red) and without (blue) fault recovery in presence of wind

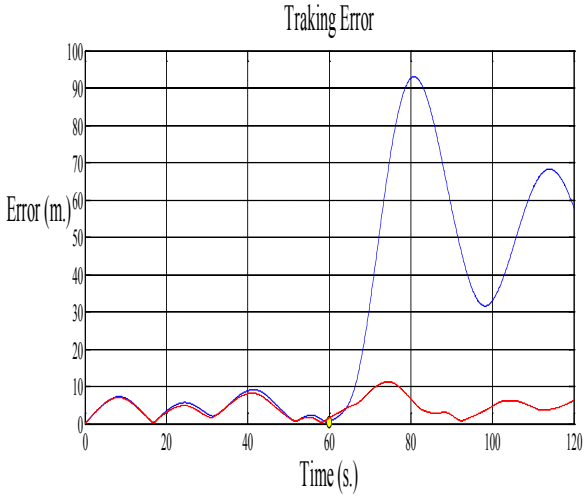

Fig. 11. Tracking error with (red) and without (blue) fault recovery in presence of wind

Finally, it is worth noting that the achieved simulation results summarized in Figs. 4-12 show the effectiveness of the presented integrated FDD and AFTCS strategy, which is able to improve the flying quality, the control objective recovery, the transient characteristics and the reference trajectory tracking when an actuator fault is acting on the aircraft model. However, the asymptotic stability of the controlled system, that in this paper are assessed in simulation, require further theoretical studies and investigations.

5. AFTCS INTEGRATED WITH FEEDBACK LINEARIZATION BASED GCS

As previously mentioned the guidance system is designed by Feedback Linearization (FL) methodology and by describing the aircraft as a point mass. Proper autopilots will realize on the rigid body the action required on the centre mass of the airplane. It is interesting to note that FL is a methodology applied usually in robotics. In aerospace application it is very unusual.

5.1 Motion Model

To spare space, throughout this section it is assumed that the reader is familiar with the concept of Feedback Linearization (FL) However the application to the three dimensional unicycle is not usual, as mentioned in the introduction, and will be treated in details. The following tri-dimensional kinematic model, well known as unicycle, will be used to develop the guidance system.

$$\begin{bmatrix} \dot{x} \\ \dot{y} \\ \dot{z} \\ \mu \\ \dot{\gamma} \end{bmatrix} = g_1(q)v + g_2(q)\omega + g_3(q)\Omega = \begin{bmatrix} \cos\mu\cos\gamma \\ \sin\mu\cos\gamma \\ \sin\gamma \\ 0 \\ 0 \end{bmatrix} v + \begin{bmatrix} 0 \\ 0 \\ 1 \\ 0 \\ 0 \end{bmatrix} \omega + \begin{bmatrix} 0 \\ 0 \\ 0 \\ 0 \\ 1 \end{bmatrix} \Omega \qquad (18)$$

$$y = \begin{bmatrix} x & y & z \end{bmatrix}^T$$

In (18) the the first three elements of the state $q = \begin{bmatrix} x & y & z & \mu & \gamma \end{bmatrix}^T$ are the three Cartesian spatial coordinate, while the last two elements are the corresponding polar angular coordinate. Obviously, the unicycle approach refers to a point mass. The output of this system is given by the three Cartesian coordinates of the point moving in a 3D space.

5.2 Controllability about a trajectory

Given a desired Cartesian trajectory motion for the unicycle model is well known that it is required the corresponding state trajectory

$$q_d = \begin{bmatrix} x_d(t) & y_d(t) & z_d(t) & \mu_d(t) & \gamma_d(t) \end{bmatrix}^T \qquad (19)$$

Must satisfy the non holomonic constraint, that is be consistent with (18). Assume that the approximate linearization of (18) is computed about $q_d(t)$. Since the linearised system is time-varying, a necessary and sufficient controllability condition is that the controllability Gramian is nonsingular. However we do not give details now, it is relatively easy to show that the previous condition is indeed satisfied as long as $v_d(t) \neq 0$ or $\omega_d(t) \neq 0$; this implies that it possible to reach a stable condition and, in particular, linear design techniques can be used to achieve local stabilization for arbitrary feasible trajectories, as long as they do not come to a stop.

5.3 Dynamic Feedback Linearization (DFL) algorithm

In the following it is illustrated the exact dynamic linearization procedure with reference to the unicycle model It will be shown that it is necessary to define an augmented system in order to obtain an overall linear system.

Differentiation of the output vector with respect to time yelds

$$\dot{\eta} \triangleq \begin{bmatrix} \dot{x} \\ \dot{y} \\ \dot{z} \end{bmatrix} = A(q) \begin{bmatrix} v \\ \omega \\ \Omega \end{bmatrix} = \begin{bmatrix} \cos\mu\cos\gamma & 0 & 0 \\ \sin\mu\cos\gamma & 0 & 0 \\ \sin\gamma & 0 & 0 \end{bmatrix} \begin{bmatrix} v \\ \omega \\ \Omega \end{bmatrix} \quad (20)$$

Showing that only v affects $\dot{\eta}$ while the angular velocities ω and Ω cannot be recovered from this first order differential information due to singularity of matrix $A(q)$. In order to proceed we need to introduce an integrator (whose state is called ξ) on the linear velocity input

$$\nu = \xi;\ \dot{\xi} = \zeta_1 \Rightarrow \dot{\eta} = \xi \begin{bmatrix} \cos\mu\cos\gamma \\ \sin\mu\sin\gamma \\ \sin\gamma \end{bmatrix} \quad (21)$$

being the new input ζ_1 the linear acceleration of the unicycle.

Thus defining the augmented system as

$$\begin{bmatrix} \dot{x} \\ \dot{y} \\ \dot{z} \\ \dot{\mu} \\ \dot{\gamma} \\ \dot{\xi} \end{bmatrix} = \begin{bmatrix} \xi\cos\mu\cos\gamma \\ \xi\sin\mu\cos\gamma \\ \xi\sin\gamma \\ 0 \\ 0 \\ 0 \end{bmatrix} + \begin{bmatrix} 0 \\ 0 \\ 0 \\ 0 \\ 0 \\ 1 \end{bmatrix} \zeta_1 + \begin{bmatrix} 0 \\ 0 \\ 0 \\ 1 \\ 0 \\ 0 \end{bmatrix} \omega + \begin{bmatrix} 0 \\ 0 \\ 0 \\ 0 \\ 1 \\ 0 \end{bmatrix} \Omega \quad (22)$$

$$y = \begin{bmatrix} x & y & z \end{bmatrix}^T$$

where $\overline{q} = \begin{bmatrix} x & y & z & \mu & \gamma & \xi \end{bmatrix}^T$ is the augmented state vector. By differentiating twice y, analogously to (20), the following new decoupling matrix $\overline{A}(\overline{q})$ is obtained

$$\overline{A}(\overline{q}) = \begin{bmatrix} \cos\mu\cos\gamma & -\xi\sin\mu\cos\gamma & -\xi\cos\mu\sin\gamma \\ -\sin\mu\cos\gamma & \xi\cos\mu\cos\gamma & -\xi\sin\mu\sin\gamma \\ \sin\gamma & 0 & \xi\cos\gamma \end{bmatrix} \quad (23)$$

and thus the output relationship

$$\ddot{\eta} = \overline{A}(\overline{q}) \begin{bmatrix} \zeta_1 \\ \omega \\ \Omega \end{bmatrix} \quad (24)$$

The matrix $\overline{A}(\overline{q})$ is non singular if $\xi \neq 0$. Under the condition, it is possible to write

$$\begin{bmatrix} \zeta_1 \\ \omega \\ \Omega \end{bmatrix} = \overline{A}^{-1}(\overline{q}) \begin{bmatrix} \ddot{x}_d(t) \\ \ddot{y}_d(t) \\ \ddot{z}_d(t) \end{bmatrix} \quad (25)$$

so as to obtain

$$\ddot{\eta} = \begin{bmatrix} \ddot{\eta}_1 \\ \ddot{\eta}_2 \\ \ddot{\eta}_3 \end{bmatrix} = \begin{bmatrix} \ddot{x}_d(t) \\ \ddot{y}_d(t) \\ \ddot{z}_d(t) \end{bmatrix} \quad (26)$$

The resulting dynamic compensator, expressed in an implicit form, is

$$\begin{bmatrix} \zeta_1 \\ \omega \\ \Omega \end{bmatrix} = \begin{bmatrix} \cos\mu\cos\gamma & -\xi\sin\mu\cos\gamma & -\xi\cos\mu\sin\gamma \\ -\sin\mu\cos\gamma & \xi\cos\mu\cos\gamma & -\xi\sin\mu\sin\gamma \\ \sin\gamma & 0 & \xi\cos\gamma \end{bmatrix}^{-1} \begin{bmatrix} \ddot{x}_d(t) \\ \ddot{y}_d(t) \\ \ddot{z}_d(t) \end{bmatrix} \quad (27)$$

In other word (27) is the inverse system of (22), so that the chain of (27) and (22), is a system with input $\begin{bmatrix} \ddot{x}_d(t) & \ddot{y}_d(t) & \ddot{z}_d(t) \end{bmatrix}$ (the second derivative of the desired trajectory) and output the actual trajectory itself. Therefore the augmented system is fully linearised resulting as the chain of two integrators for each element of the output vector.

5.4 Functional conditions

The dynamic compensator, as already noticed, has a potential singularity at $\xi = \nu = 0$ *i.e.*, when the unicycle is not moving. This difficulty must be taken into account when designing control laws on the equivalent linear model, but in case of aircrafts this condition cannot obviously occur. Anyway there is another functional condition that must be taken into account to enable the correct behaviour of the guidance system.

The dynamic compensator and the aircraft must be initialized perfectly as the same condition; even a small difference can cause a complete wrong generation of input by the dynamic compensator. To avoid this strict condition, as we will show further in the paper, an external position feedback has been developed.

5.5. Interaction architecture

It's now well known how the guidance system generates its output, which are in particular the kinematic quantities of: linear velocity modulus v and two angular velocities ω and Ω. It is either well known that commonly classical autopilots do not accept such an input, thus the two angular velocity signal must be converted in the correspondent angles ψ and γ by simple integration. Therefore it is really easy to relate the dynamic compensator of the Feedback Linearization with standard autopilots of the airplane. Anyway the problem is only shifted on the autopilot architecture; its role, in fact, is to make the stabilized airplane as close as possible to the unicycle. In the sketch below the complete architecture of the GCS is shown, and the equivalence assumption and consequent substitution between unicycle and aircraft is highlighted.

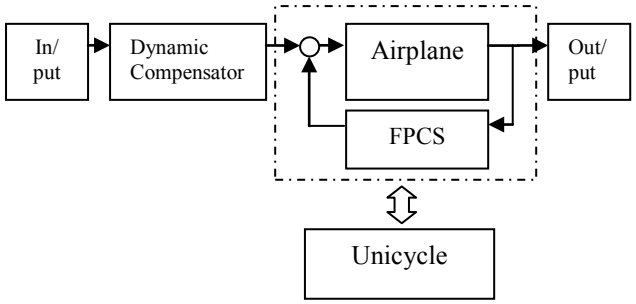

Fig. 12. Integrated design of Guidance and Control system

where FPCS denote a Flight Path Control System. The dynamic compensator consist in (27) plus the integral operation that leads to ψ and γ. The input is the second derivative of the desired trajectory and the output is the actual trajectory. From a general point of view of linear autopilots, for almost every kind of aircraft the information generated by the dynamic compensator can be managed through the usage of a "velocity and altitude hold", about the longitudinal flight quantities, and the usage of a "heading hold", about the lateral ones. In order to use this structure the guidance input γ has to be transformed in the absolute height that is the reference input for the "altitude hold". Taking in mind that the dynamic compensator is originally developed on a unicycle model, which implies no "slippage", also the aircraft should have the same motion constrains, and in order to do this it is necessary to add a "zero lateral side-force" autopilot.

5.6 Autopilots definitions

A fundamental requirement for a FPCS is that the asymptotic tracking error

$$\lim_{t\to\infty}\left(\begin{bmatrix} x(t)-x_d(t) & y(t)-y_d(t) & z(t)-z_d(t)\end{bmatrix}^T\right) \quad (28)$$

should be close to zero. In this paper we take in account only a small class of the wide referenced autopilot, the "classical autopilots" that are mostly diffused in the general aviation aircrafts. Anyway, it is obviously possible to use different techniques concerning the FPCS of Fig. 11, but it has to be denoted that in the conceptual idea of the integration proposed nothing really changes. Moreover, as well known, in order to have null asymptotic tracking error with a certain degree of robustness, the FPCS must provide a proportional plus integral state feedback. We do not give details now about the development of this type of the FPCS, that is designed on the basis of the proportional plus integral linear quadratic (LQ) optimal control as described in Anderson and Moore (1990).

With reference to the results obtained just above, we can show a good feature of the GCS proposed. It is possible with a few operations to set-up the autopilots in order to catch perfectly the requirement imposed by the reference trajectory, avoiding late responses or, on the other side, too fast and useless response dynamic of the autopilot, that can also negatively affect the global flight qualities of the airplane. Thus in addition to the great flexibility in variety of trajectories, we have shown that almost the same flexibility is available for the research of the best performance of the autopilots.

At last there is another characteristic that must be highlighted of the chosen FPCS architecture, the system can reject several faults that can occur at the command surfaces. For example a step error on the effective elevator surface will be recovered in a finite transient. So that this type of autopilots is useful in order to show the effectiveness of the AFTC scheme proposed in the previous chapters. It will be shown how the performance in the transient response of the aircraft to the fault are improved.

5.6 Position feedback

In order to make the global guidance and control system robust to external disturbances and to non perfect initialization of the flight parameters. It is useful to provide the guidance system with the following position and velocities errors feedback

$$\begin{cases} \ddot{x}_{ref} = \ddot{x}_d + K_{\mathrm{p}x}\left(x_d - x\right) + K_{\mathrm{d}x}\left(\dot{x}_d - \dot{x}\right) \\ \ddot{y}_{ref} = \ddot{y}_d + K_{\mathrm{p}y}\left(y_d - y\right) + K_{\mathrm{d}y}\left(\dot{y}_d - y\right) \\ \ddot{z}_{ref} = \ddot{z}_d + K_{\mathrm{p}z}\left(z_d - z\right) + K_{\mathrm{d}z}\left(\dot{z}_d - z\right) \end{cases} \quad (29)$$

where the subscript *ref* denote the commanded acceleration to the dynamic compensator.
It this way the input of the dynamic compensator of Figure 11 is described by (29). Obviously thanks to the Feedback Linearization, the gains in (29) can be computed by means of linear methodologies.

5.7 Simulation Results

In this section the results obtained by exploiting the guidance and control system described in the previous sub section of section 5 are proposed. The simulation conditions are the same of section 4 with the difference that the fault affects the

rudder. The fault size is 3 degree. It is worth recalling that the time needed to perform the whole circumference is exactly 120 sec so that the proposed figures regard the whole turn.

Only the most meaningful figures referring to the case with presence of wind are proposed to spare space. In Fig. 12 it is shown the correct estimation of the rudder actuator fault. Oscillation are due to the presence of wind.

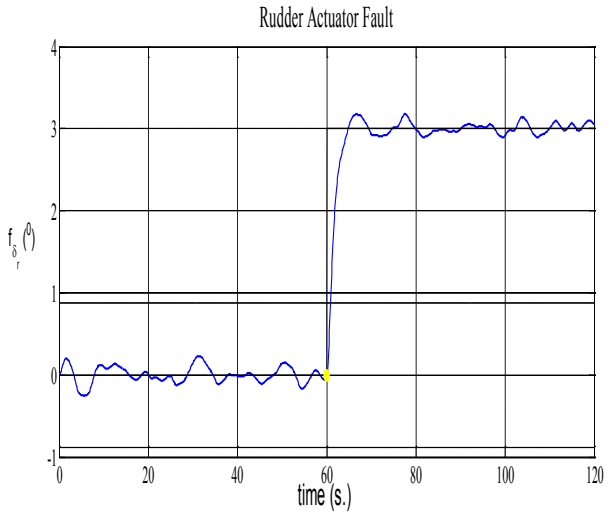

Fig. 13. Estimated rudder actuator fault in presence of turbulence

In the following figure the tracking error due to a rudder fault occurring in the middle of the coordinated turn is shown. It is possible to observe the better performances of the guidance and control system obtainable by means of the proposed AFTCS.

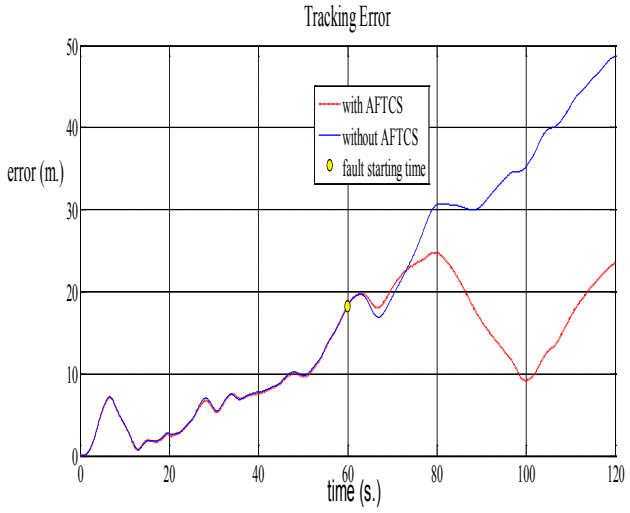

Fig. 14. Tracking error with and without AFTCS in presence of turbulence.

It is useful to denote that after time 120 sec, not shown in Fig. 13 that regards one single turn, both the tracking error stabilize toward constant values. The case with AFTCS is still characterized by the better performance.

6. CONCLUSIONS

This paper described the development of a novel active fault tolerant control scheme, which integrates a robust fault diagnosis scheme with the design of a controller reconfiguration system. The methodology was based on a fault detection and diagnosis procedure relying on adaptive filters designed via the nonlinear geometric approach. The novelty of the proposed fault tolerant scheme consisted of the use of the fault signal estimated by these adaptive filters and exploited in the closed loop scheme for improving the performances of the overall system.

The fault tolerant strategy was tested on the PA-30 aircraft simulator in a challenging flight condition, in the presence of actuator faults and turbulence. Moreover the simulations regards also the use of two different guidance system applied to the aircraft simulator. If the first one is a classic guidance design, the second one, proposed in section 5, is a novel application of methods coming from robotics (Feedback Linearization) and it has capabilities of fault rejection, combined with high flexibility and good tracking accuracy. Anyhow, as shown by simulations, the AFTCS structure improves the global guidance performance in the occurrence of a fault even for latter GCS. Further investigations will regard the proof of the stability of the overall fault tolerant scheme and the application with real data.

REFERENCES

Anderson B.D.O. and Moore J.B. (1990)). In *Optimal Control – Linear Quadratic Methods*. Prentice Hall Information and Systems Sciences Series, chap. 9. Englewood Cliffs, New Jersey.

Blanke, M., Kinnaert, M., Lunze, J. and Staroswiecki, M. (2006). *Diagnosis and Fault-Tolerant Control*. Springer - Verlag.

Bonfè, M., Castaldi, P., Geri, W. and Simani, S (2006). Fault Detection and Isolation for On-Board Sensors of a General Aviation Aircraft. *International Journal of Adaptive Control and Signal Processing*, 20(8), 381-408.

Bonfè, M., Castaldi, P., Geri, W. and Simani, S (2007a). Design and Performance Evaluation of Residual Generators for the FDI of an Aircraft. *International Journal of Automation and Computing*, 4(2), 156-163.

Bonfè, M., Castaldi, P., Geri, W. and Simani, S (2007b). Nonlinear Actuator Fault Detection and Isolation for a General Aviation Aircraft. *Space Technology - Space Engineering, Telecommunication, Systems Engineering and Control*, 27(2&3), 107-113.

Bonfè, M., Castaldi, P., Geri, W., Simani, S. and Benini, M. (2007). Design and Performance Evaluation of Fault Diagnosis Strategies for a Simulated Aircraft Nonlinear Model. *Journal of Control Science and Engineering*. 2008, 1-18.

Castaldi, P., Geri, W., Bonfè, M., Simani, S. and Benini, M. (2009). Design of residual generators and adaptive filters for the FDI of aircraft model sensors. *Control Engineering Practice* (printing, available on linehttp://dx.doi.org/10.1016/j.conengprac.2008.11.006)

Chen J. and Patton R. J. (1999). *Robust Model–Based Fault Diagnosis for Dynamic Systems*. Kluwer Academic Publishers.

De Persis, C. and Isidori, A. (2001). A geometric approach to non linear fault detection and isolation. *IEEE Transactions on Automatic Control*, 45(6), 853–865.

Fink, M.P. and Freeman Jr D.C.(1969). Full-scale wind-tunnel investigation of static longitudinal and lateral characteristics of a light twin-engine airplane. *Technical Report* TN D-4983. NASA.

Koziol, Jr J.S. (1971). Simulation model for the PIPER PA-30 light maneuverable aircraft in the final approach. *Technical Report* DOT-TSC-FAA-71-11. NASA.

Ioannou, P. and Sun, J. (1996). *Robust Adaptive Control*. Upper Saddle River, NJ, USA: PTR Prentice–Hall.

Isermann, R. (2005). *Fault–Diagnosis Systems: An Introduction from Fault Detection to Fault Tolerance*, 1st ed. Springer - Verlag.

Mahmoud, M., Jiang, J and Zhang, Y. (2003). *Active Fault Tolerant Control Systems*. Springer-Verlag.

Marcos, A., Ganguli, S. and Balas, G. J. (2005). An application of h_∞ fault detection and isolation to a transport aircraft. *Control Engineering Practice*, 13, 105 - 119.

Moorhouse D and Woodcock (1980). R. U.S. Military Specification MIL-F-8785C. *Technical Repo*rt, U.S. Department of Defense.

Ojha, S.K.(1995) *Flight Performance of Aircraft*. AIAA Aerospace Educational Series. AIAA: New York.

Simani, S., Fantuzzi, C. and Patton R.J .(2002). *Model-based fault diagnosis in dynamic systems using identification techniques*, 1st ed. Ser. Advances in Industrial Control. Springer–Verlag..

Stevens, B. L. and Lewis, F. L. (2003). *Aircraft Control and Simulation*. 2nd ed. John Wiley and Son.

Witczak, M. (2007). *Modelling and Estimation Strategies for Fault Diagnosis of Non–Linear Systems: From Analytical to Soft Computing Approaches*, 1st ed. Ser. Lecture Notes in Control & Information Sciences. Springer-Verlag.

Zhang, Y. and Jiang, J. (2008). "Bibliographical review on reconfigurable fault tolerant control systems," *Annual Reviews in Control*, 32, 229– 252.

APPENDIX A

$$
\begin{cases}
\dot{V} &= -\dfrac{\left(C_{D0}+C_{D\alpha}\alpha+C_{D\alpha_2}\alpha^2\right)}{m}V^2+n+\\
&\quad +g\left(\sin\alpha\cos\theta\cos\phi-\cos\alpha\sin\theta\right)+n+\\
&\quad +\dfrac{\cos\alpha}{m}\dfrac{t_p}{V}\left(t_0+t_1n_e\right)\delta_{th}+w_v\sin\alpha\\
\dot{\alpha} &= -\dfrac{\left(C_{L0}+C_{L\alpha}\alpha\right)}{m}V+n+\\
&\quad +\dfrac{g}{V}\left(\cos\alpha\cos\theta\cos\phi+\sin\alpha\sin\theta\right)+q_\omega+\\
&\quad +n+-\dfrac{\sin\alpha}{m}\dfrac{t_p}{V^2}\left(t_0+t_1n_e\right)\delta_{th}+\dfrac{\cos\alpha}{V}w_v\\
\dot{\beta} &= \dfrac{\left(C_{D0}+C_{D\alpha}\alpha+C_{D\alpha_2}\alpha^2\right)\sin\beta+C_{Y\beta}\beta\cos\beta}{m}V\\
&\quad +n+g\dfrac{\cos\theta\sin\phi}{V}+p_\omega\sin\alpha-r_\omega\cos\alpha+n+\\
&\quad -\dfrac{\cos\alpha\sin\beta}{m}\dfrac{t_p}{V^2}\left(t_0+t_1n_e\right)\delta_{th}+\dfrac{1}{V}w_\ell\\
\dot{p}_\omega &= \dfrac{\left(C_{l\beta}\beta+C_{lp}\,p_\omega\right)}{I_x}V^2+\dfrac{\left(I_y-I_z\right)}{I_x}q_\omega r_\omega+\dfrac{C_{\delta_a}}{I_x}V^2\delta_a\\
\dot{q}_\omega &= \dfrac{\left(C_{m0}+C_{m\alpha}\alpha+C_{mq}\,q_\omega\right)}{I_y}V^2+\dfrac{\left(I_z-I_x\right)}{I_y}p_\omega r_\omega+\\
&\quad +n+\dfrac{C_{\delta_e}}{I_y}V^2\delta_e+\dfrac{t_d}{I_y}\dfrac{t_p}{V}\left(t_0+t_1n_e\right)\delta_{th}\\
\dot{r}_\omega &= \dfrac{\left(C_{n\beta}\beta+C_{nr}\,r_\omega\right)}{I_z}V^2+\dfrac{\left(I_x-I_y\right)}{I_z}p_\omega q_\omega+\dfrac{C_{\delta_r}}{I_z}V^2\delta_r\\
\dot{\phi} &= p_\omega+\left(q_\omega\sin\phi+r_\omega\cos\phi\right)\tan\theta\\
\dot{\theta} &= q_\omega\cos\phi-r_\omega\sin\phi\\
\dot{\psi} &= \dfrac{\left(q_\omega\sin\phi+r_\omega\cos\phi\right)}{\cos\theta}\\
\dot{n}_e &= t_n n_e^3+\dfrac{t_f}{n_e}\left(t_0+t_1n_e\right)\delta_{th}
\end{cases}
\tag{30}
$$

where $C_{(\cdot)}$ are the aerodynamic coefficients; $t_{(\cdot)}$ are the engine parameters; w_w, w_v are the vertical and lateral wind disturbance components respectively.